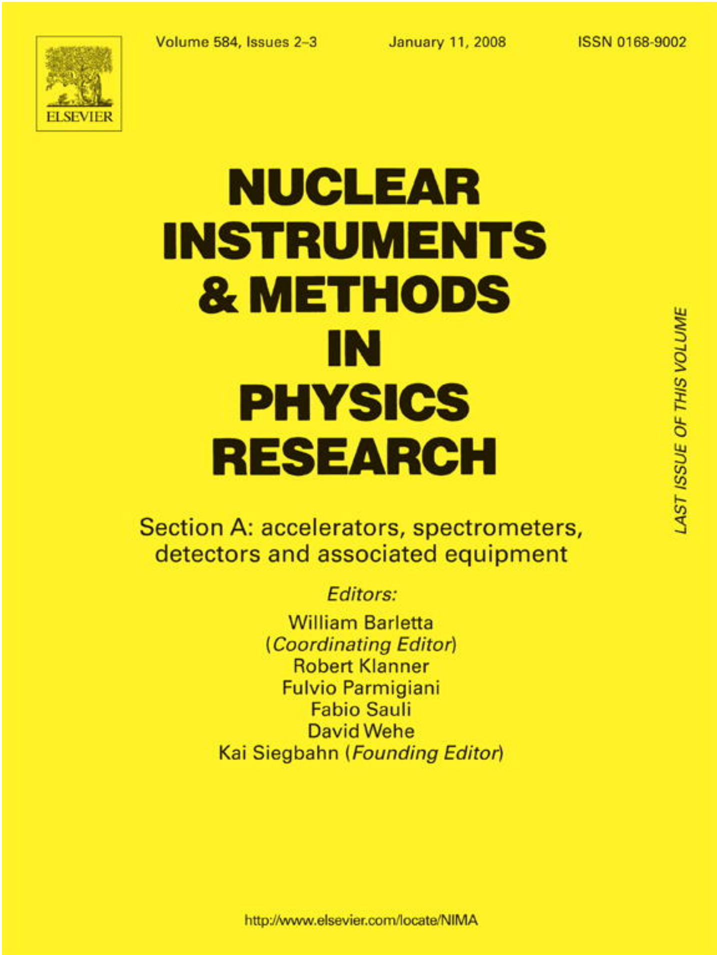
Volume 584, Issues 2–3
January 11, 2008
ISSN 0168-9002
ELSEVIER
NUCLEAR INSTRUMENTS & METHODS IN PHYSICS RESEARCH
Section A: accelerators, spectrometers, detectors and associated equipment
Editors:
William Barletta (Coordinating Editor)
Robert Klanner
Fulvio Parmigiani
Fabio Sauli
David Wehe
Kai Siegbahn (Founding Editor)
LAST ISSUE OF THIS VOLUME
http://www.elsevier.com/locate/NIMA

Available online at www.sciencedirect.com
ScienceDirect
Nuclear Instruments and Methods in Physics Research A 584 (2008) 377–382
NUCLEAR INSTRUMENTS & METHODS IN PHYSICS RESEARCH Section A
www.elsevier.com/locate/nima

Deep inelastic neutron scattering on ^{207}Pb and $NaHF_2$ as a test of a detectors array on the VESUVIO spectrometer

A. Pietropaolo*, R. Senesi

Università degli Studi di Roma Tor Vergata, Dipartimento di Fisica and Centro NAST (Nanoscienze & Nanotecnologie & Strumentazione), via della Ricerca Scientifica 1, 00133 Roma, Italy

Received 17 August 2007; received in revised form 3 October 2007; accepted 4 October 2007
Available online 22 October 2007

Abstract

A prototype array of resonance detectors for deep inelastic neutron scattering experiments has been installed on the VESUVIO spectrometer, at the ISIS spallation neutron source. Deep inelastic neutron scattering measurements on a reference lead sample and on $NaHF_2$ molecular system are presented. Despite on an explorative level, the results obtained for the values of mean kinetic energy $\langle E_k \rangle$ are found in good agreement with the theoretical predictions, thus assessing the potential capability of the device for a routine use on the instrument.

PACS: 28.52.Lf; 29.30.Kv; 29.40.Wk

Keywords: Scintillator detectors; Neutron instrumentation; Neutron scattering

1. Introduction

Deep inelastic neutron scattering (DINS) is a unique experimental technique providing information on the short-time dynamics of nuclei in condensed matter systems [1–3]. A remarkable development of the technique occurred since middle eighties, when intense fluxes of epithermal neutrons were made available from spallation pulsed neutron sources. Inverse geometry spectrometers (i.e. instruments where the final neutron energy is selected) operating at pulsed neutron sources can reach unlimited energy (loss), $\hbar\omega$, and wave vector, q, transfers. Indeed, the higher the selected neutron energy, the larger the values of $\hbar\omega$ and q achievable in the scattering measurements. On these instruments, the only effective way to select neutron energies above 1 eV is to use nuclear resonances which on one hand allow energy analysis up to several tens of eV, on the other pose technological problems related to the neutron counting method. As a matter of fact, the standard neutron detectors based on scintillation materials (Li-glass(Ce) or ZnS(Ag)) and/or gas counters (^{3}He tubes) at different pressures (1–20 atm), show an efficiency that decreases as $1/v, v$ being the neutron velocity. An advantage for an inverse geometry instrument is the possibility to use of the so-called Resonance Detector (RD) configuration, proposed between the end of 1970s and the beginning of 1980s [4–14], and developed in the last years [15–21] for the VESUVIO spectrometer [22] (ISIS spallation neutron source, United Kingdom). In the RD configuration, neutrons are revealed by using a detection system composed of an analyzer foil, made of a material such as ^{238}U or ^{197}Au, and a photon detector. The analyzer selects the energy of the scattered neutrons through (n,γ) resonance reactions, while the photon detector registers the prompt radiative capture gamma-rays. Experimental investigations carried out on the VESUVIO spectrometer have shown the great capability of cerium-activated yttrium–aluminium–perovskite (YAP) scintillators in terms of efficiency and signal to background (S/B) ratio enhancement [19].

A recent development for DINS measurements on VESUVIO is the Foil Cycling Technique (FCT) [23],

*Corresponding author. Tel.: +39 672594549; fax: +39 62023507.
E-mail addresses: antonino.pietropaolo@roma2.infn.it, pietropaolo@roma2.infn.it (A. Pietropaolo).

0168-9002/$ - see front matter © 2007 Elsevier B.V. All rights reserved.
doi:10.1016/j.nima.2007.10.028

which was found to improve the spectrometer resolution, providing an appreciable counting efficiency and a good neutron and gamma background subtraction method [23,24].

After several tests on different detectors and pilot DINS experiments on a variety of samples, employing both the RD and the FCT configurations on VESUVIO, a prototype array of resonance detectors was developed and installed in order to investigate the possibility of a routine use of the RD configuration on the instrument.

In this paper, DINS measurements on a polycrystalline ^{207}Pb reference sample and on the $NaHF_2$ molecular system are presented. The measurements have been carried out in the RD configuration, employing the prototype array of YAP-based RD units and the FCT. It has to be stressed that these experiments represent the first attempt to use the RD configuration and the FCT with an array of detectors. Indeed, previous measurements with the FCT were performed by using only one or a couple of RD units [23]. The aim is a preliminary investigation of the capabilities of such a device, for a routine use in the user research program of the VESUVIO instrument.

This paper is organized as follows: In Section 2, the experimental set up of the two measurements is presented, while in Section 3 the results are discussed. In Section 4, the conclusions are drawn, while in the Appendix section the DINS basic theory and the RD configuration are briefly discussed.

2. Experiment

The DINS measurements have been carried out on the VESUVIO spectrometer operating at the ISIS spallation source. The layout of the instrument is schematically shown in Fig. 1. The incident neutron beam, from a water moderator at ambient temperature, is characterized by a white energy spectrum, resulting in a peak at about 0.03 eV and a $E_0^{-0.9}$ tail in the epithermal region, E_0 being the incident neutron energy. The RD detection system consisted of an array of 32 YAP scintillators, coupled to ^{197}Au analyzer foils. In order to employ the FCT, a cycling foil was attached to the moving frame surrounding the sample tank and cycled in and out of the scattered neutron beam. For more experimental and theoretical details about the FCT, the reader is referred to Refs. [23,24].

Each element of the array was a YAP crystal (80 mm × 25 mm area and 6 mm thickness) facing a 12.5 μm thick gold analyzer, having the same area of the scintillator. The latter was coupled by means of a light guide to a photomultiplier tube and then to the electronics. The whole array covered an angular range of about 20° (from 40° to 60°) at an average distance $\langle L_1 \rangle \simeq 70$ cm from the sample position. The cycling foil (10 cm × 10 cm × 12.5 μm gold foil) was placed at a distance of about 40 cm from the array.

In this set up, a polycrystalline lead (^{207}Pb) sheet 100 cm^2 area and 1 mm thickness was used as scattering sample for a first set of DINS measurements. ^{207}Pb is routinely used for calibration purposes on the instrument, as its response function is well known. Thus, it can be considered as an important test sample to assess the performances of the detectors array.

A second set of DINS measurements was performed on a sodium hydrogen fluoride ($NaHF_2$) sample at $T = 4$ K, formed by an array of small polycrystalline platelets placed on a thin aluminum frame. For these measurements, VESUVIO was equipped with two sets of ^{197}Au cycling foils and four banks of YAP detectors, ranging between $2\vartheta = 45°$ and $2\vartheta = 62.3°$ on both sides of the spectrometer.

An example of a raw DINS time of flight (TOF) spectrum from ^{207}Pb is shown in Fig. 2, while Fig. 3 shows three DINS spectra from $NaHF_2$ acquired by detectors placed at different scattering angles in the array. The latter plot clearly exhibits two recoil peaks: a broad and large feature on the left, produced by the hydrogen ions (H+), and a narrower structure determined by all the heavier elements: fluorine (F−), sodium (Na+) and aluminum (Al), the latter being contained in the sample holder frame. The time shift among the three different H recoil peaks shown in the figure is due to the different energy and wave vector transfers achieved at the different scattering angles.

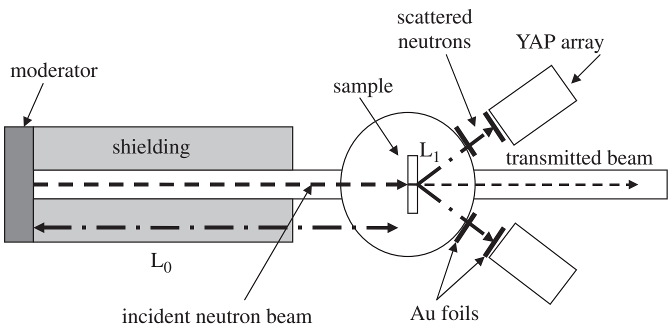

Fig. 1. Schematic layout of the VESUVIO spectrometer for DINS measurements.

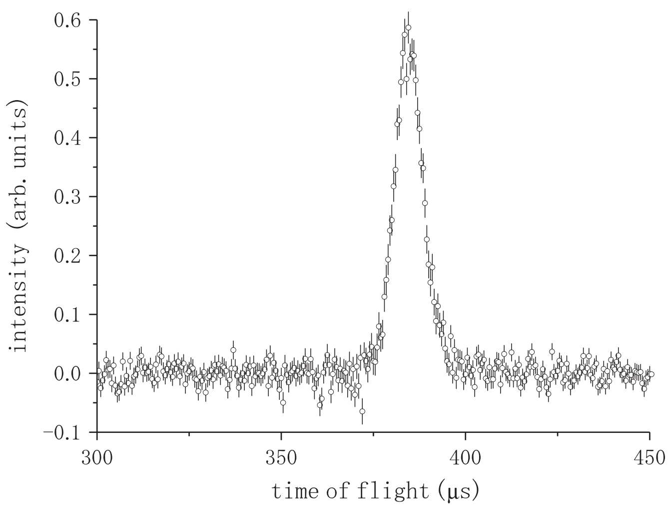

Fig. 2. DINS time of flight spectrum with statistical error bars from a ^{207}Pb sample, acquired by a detector placed at a scattering angle $2\vartheta = 50°$.

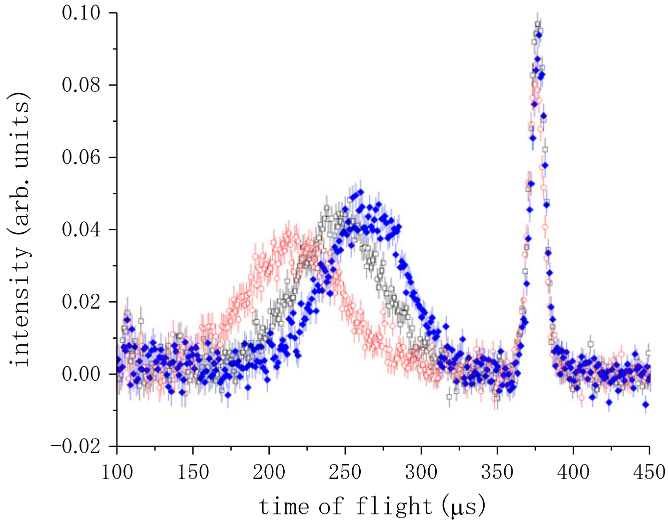

Fig. 3. (color on line) DINS time of flight spectra with statistical error bars from a $NaHF_2$ molecular system, acquired by detectors placed at $2\vartheta = 48^\circ$ (full diamonds), 52° (empty squares) and 56° (empty circles): the peaks at about 375 μs are the recoil signals of Al + Na + F nuclei, while the peaks in the region 225–260 μs are the H recoil signals.

In the case of ^{207}Pb DINS spectra, it has to be noted that the FCT provides an appreciable background subtraction in the whole TOF range. In the $NaHF_2$ case, as already observed in previous measurements employing the FCT [23], the background subtraction is satisfactory even in the region between the H recoil peak and the Al + F + Na peak at almost all scattering angles. This and the narrowing of the resolution [23,24] are very important when a fine recoil lineshape analysis is required.

3. Results

From the TOF spectra shown in Figs. 2 and 3 it is possible to obtain for each detector, through standard procedures, the so-called Experimental Compton Profile, given by the convolution of the Neutron Compton Profile (NCP), $J(y)$, and the resolution function of the instrument for the considered detector (see Appendix section for more details and refer to Ref. [20] for a thorough description of RD data analysis).

In the case of ^{207}Pb sample, a simulation of the response functions of each detector of the array has been carried out by using a modified version of the DINSMS code, developed by Mayers and co-workers [25]. Fig. 4 shows the comparison between the experimental TOF data acquired by a single detector placed at a scattering angle of about 45°, and the corresponding simulated spectrum. The simulation was performed imposing a $J(y)$ of Gaussian shape and standard deviation $\sigma_{Pb} = 35.3\,Å^{-1}$. This value (and lineshape), as already stressed above, is well assessed as lead is used for calibration purposes in DINS measurements on VESUVIO. The agreement between experimental and simulated data is good, with a χ^2 value of about 1.2. By considering the whole set of detectors, the overall

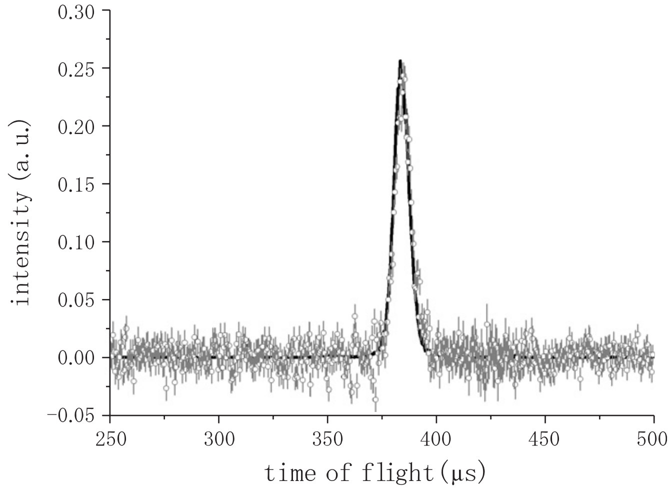

Fig. 4. Experimental DINS time of flight spectrum with statistical error bars (open dots) from ^{207}Pb scatterer at $2\vartheta = 45^\circ$ and corresponding simulated data (continuous line).

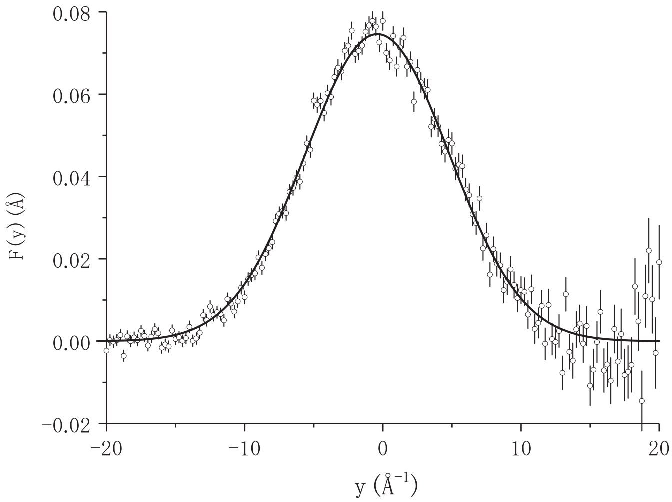

Fig. 5. Experimental Compton Profile (see Appendix for details) with statistical error bars, obtained by transformation in the y space of time of flight spectra acquired by two detectors placed at equal (within 1°) scattering angle. The continuous line represents a fit obtained employing a simple Gaussian $J(y)$.

agreement between experimental and simulated spectra is still quite satisfactory, with an average chi-squared $\langle\chi^2\rangle \simeq 1.4$.

A simultaneous fit over the whole set of $NaHF_2$ spectra was performed, within the framework of the Convolution Approximation [20], using a code based on a Fortran 77 routine, employing a MINUIT package [27] for χ^2 minimization. The resolution functions were calculated using the standard calibration procedures employed on the instrument [26]. The simultaneous fit envisaged the use of a single $J(y)$ convoluted with the resolution function of each detector of the array (see Ref. [20] for details). The simultaneous fit over 32 spectra (reduced to 16 by summing signals from detectors placed at equal scattering angles within 1°) allowed to obtain an overall statistics which is a factor of about 5 better than the one achieved on a single spectrum. By using a simple Gaussian form for the proton NCP, $J(y)$, the fit procedure provided a value of $\sigma_H = 4.24 \pm 0.02\,\text{Å}^{-1}$ (the uncertainty being calculated by the error analysis of the minimization routine) corresponding to a mean kinetic energy $\langle E_k \rangle = 112 \pm 1\,\text{meV}$, with a $\chi^2 = 1.3$. This value is found to be in agreement within 10% with the value expected from lattice dynamics simulations ($\langle E_k \rangle \simeq 123\,\text{meV}$) [28]. The discrepancy may be explained by considering that a Gaussian line shape does not take into account possible anharmonic contribution of the momentum distribution. Fig. 5 shows the experimental proton NCP, obtained by the weighted sum of two spectra acquired by two detectors at equal (within 1°) scattering angle, and the corresponding fit.

4. Conclusions

Deep inelastic neutron scattering measurements on a ^{207}Pb reference sample and on $NaHF_2$ molecular crystals have been performed on the VESUVIO spectrometer at the ISIS spallation neutron source. The Foil Cycling Technique has been employed with a prototype array of resonance detectors, based on YAP scintillators crystals coupled to gold analyzer foils.

The aim of the present measurements was to investigate the potential capability of the prototype array to serve as a stable equipment for DINS experiments on VESUVIO.

The experimental DINS data from ^{207}Pb were compared to simulations, while the whole set of $NaHF_2$ spectra was simultaneously fitted by employing a simple Gaussian model for the proton Neutron Compton Profile.

It has to be noted that, as already shown by previous simulations employing the GEANT4 package [29], the cross talk between adjacent crystals should be as low as 5–10%. Further experimental studies as well as simulations on the prototype array will be devoted to a fine assessment of the cross talk level and to test other possible configurational arrangements for resolution and efficiency improvements.

As a matter of fact, the results obtained for momentum distribution and mean kinetic energy of both ^{207}Pb and $NaHF_2$ samples, investigated in this experimental work, are in good agreement with theoretical predictions, thus showing the potential capability of this prototype device for DINS measurements on VESUVIO.

Acknowledgements

This work was supported within the CNR-CCLRC Agreement No. 01/9001 concerning collaboration in scientific research at the spallation neutron source ISIS. The financial support of the Consiglio Nazionale delle Ricerche in this research is hereby acknowledged. The authors greatly acknowledge E.M. Schooneveld (ISIS facility) for fruitful discussions and M.A. Adams (ISIS facility) for continuous collaboration during the measurements on VESUVIO. Dr. J. Mayers (ISIS facility) and Dr. D. Colognesi (Consiglio Nazionale delle Ricerche, Italy) are acknowledged for great collaboration in data analysis on $NaHF_2$.

Appendix A

A.1. DINS theoretical framework

In the DINS regime, the inelastic neutron scattering cross section for unpolarized neutrons is related to the dynamic structure factor $S(\mathbf{q},\omega)$ via the relation [30,31]:

$$\frac{d^2\sigma(E_0,E_1,2\vartheta)}{d\Omega\, dE_1} = \hbar^{-1}\sqrt{\frac{E_1}{E_0}}[|b|^2 S(\mathbf{q},\omega) + (|b^2| - |b|^2) S_I(\mathbf{q},\omega)] \quad (1)$$

b being the scattering length of the probed nucleus, $S_I(\mathbf{q},\omega)$ is the incoherent contribution to the total dynamic structure factor, while E_0, E_1 are the incident and final neutron energies and 2ϑ the scattering angle, respectively.

At high q values (typically above $20\,\text{Å}^{-1}$), the scattering is incoherent, that is it occurs from single a particle, since the spatial correlations between different atoms being negligible, due to the exceedingly low values of the Debye–Waller factors involved.

The typical values of the energy transfer $\hbar\omega$ attainable in DINS experiments in the $20° \leqslant 2\vartheta \leqslant 170°$ interval (from intermediate to backscattering angles) range between 1 and 100 eV, corresponding to time scales in the order of 10^{-15}–10^{-17} s. These are much shorter than the characteristics times of the high energy collective modes in condensed matter (typically well above $\tau \simeq 10^{-15}$ s for the most energetic modes like molecular stretching). Under these kinematical conditions, the nucleus probed by the neutron recoils freely [1,2]. Thus, DINS explores the so-called short-time self dynamics and the incoherent and free recoil scattering (resembling the Compton scattering of hard X-rays off electrons) manifest in the well-known Impulse Approximation (IA). Within the IA, the inelastic neutron scattering cross-section in Eq. (1) is

$$\frac{d^2\sigma(E_0,E_1,2\vartheta)}{d\Omega\, dE_1} = \hbar^{-1}\sqrt{\frac{E_1}{E_0}}[|b^2| S_{IA}(\mathbf{q},\omega)]. \quad (2)$$

The dynamic structure factor is given by

$$S_{IA}(\mathbf{q},\omega) = \hbar \int n(\mathbf{p})\delta\left[\hbar\omega - \hbar\omega_r - \frac{\mathbf{p}\cdot\hbar\mathbf{q}}{M}\right] d\mathbf{p}. \quad (3)$$

Eq. (3) states that scattering occurs between the neutron and a single particle, with conservation of kinetic energy and momentum of the particle + neutron system. The term $\hbar\omega_r = \hbar^2 q^2/2M$ is the recoil energy, i.e. the kinetic energy the struck particle would have, providing it were stationary before the collision and absorbed all the momentum transferred by the neutron. Within the framework of the IA, $\hbar\omega$ and q are explicitly coupled through the scaling variable y, defined as [30]

$$y = \frac{M}{\hbar^2 q}(\hbar\omega - \hbar\omega_r). \tag{4}$$

Eq. (3) can then be reduced to the form

$$S_{\mathrm{IA}}(\mathbf{q},\omega) = \frac{M}{\hbar q} J(y,\hat{q}) \tag{5}$$

where

$$J(y,\hat{q}) = \hbar \int n(\mathbf{p}')\delta(\hbar y - \mathbf{p}' \cdot \hat{q})\,\mathrm{d}\mathbf{p}' \tag{6}$$

$J(y,\hat{q})$ being the Neutron Compton Profile (NCP), formally defined as the Radon transform of the momentum distribution. The quantity $\hat{q}$ is a unit vector, as $J(y,\hat{q})$ no longer depends on the magnitude of $\mathbf{q}$. The function $J(y,\hat{q})\,\mathrm{d}y$ is the probability for an atom to have a momentum parallel to $\hat{q}$ of magnitude between $\hbar y$ and $\hbar(y+\mathrm{d}y)$.

For an isotropic system, the dependence on $\hat{q}$ can be dropped, and Eq. (6) becomes

$$J(y) = 2\pi\hbar \int_{|\hbar y|}^{\infty} p n(p)\,\mathrm{d}p. \tag{7}$$

The relation between $n(p)$ and $J(y)$ is then [1]

$$n(p) = -\frac{1}{2\pi\hbar^3 y} \cdot \left(\frac{\mathrm{d}J(y)}{\mathrm{d}y}\right)_{\hbar y = p}. \tag{8}$$

The asymptotic formula of Eq. (5) is in practice never attained, since IA implies the unphysical double limit $(q,\hbar\omega) \to \infty$, keeping $y = \mathrm{const}$. For this reason Eq. (5) is generally replaced by

$$S_s^{(n)}(\mathbf{q},\omega) = \frac{M_n}{\hbar q} F_n(y_n,\mathbf{q}) \tag{9}$$

where $F_n(y_n,\mathbf{q})$ retains an additional dependence on q, irreducible to the West scaling. Such a dependence is generally known as Final State Effects (FSE) [2]. Various methods for the approximate evaluation of FSE have been devised so far [32–36], the simplest and most widely used of which being the so-called additive approach [32,37].

A.2. The RD configuration

The RD counting procedure relies upon two main steps [15,17]: in the first one, the scattered neutron beam impinges onto the analyzer foil which provides the energy analysis by means of (n, γ) resonance absorption at a given resonance energy E_1; in the second step, the prompt gamma-rays are detected to assign the total neutron time of flight.

It has to be stressed that the gamma detector is used as a counter. For each absorbed neutron into the analyzer, the production of a gamma-ray cascade occurs. It is enough that one photon among the whole cascade is detected, even by a partial release of its energy in the detector's active medium, to trigger a stop (i.e. counting) signal for the electronics.

The experimental signal recorded in the RD configuration is a time of flight spectrum, representing the number of counts collected in a time channel of width δt centered in t. The count rate per time bin is given by the expression [38]:

$$C(t,\langle 2\vartheta\rangle) = \beta \cdot I_P \int_0^{\infty} \mathrm{d}E_0 \Phi(E_0) \int_0^{\infty} \mathrm{d}E_1 \times (1 - T(E_1))\delta(\tau)\left(\frac{\mathrm{d}^2\sigma}{\mathrm{d}\Omega\,\mathrm{d}\hbar\omega}\right) \tag{10}$$

where β is given by

$$\beta = n_T \Delta\Omega \rho_s d_s \eta. \tag{11}$$

I_P is defined as

$$I_P = \int_{-\infty}^{\infty} \mathrm{d}t_0 \int_0^{\pi} \mathrm{d}(2\vartheta) \int_0^{\infty} \mathrm{d}L_0 \times \int_0^{\infty} \mathrm{d}L_1 P(t_0, 2\vartheta, L_0, L_1) \tag{12}$$

and the argument in the δ-function is

$$\tau = \left(t - t_0 - L_0\sqrt{\frac{m_n}{2E_0}} - L_1\sqrt{\frac{m_n}{2E_1}}\right). \tag{13}$$

In the previous set of Eqs. (10)–(13), m_n is the neutron mass, n_T is the number of neutron pulses included in the measurement, $\Delta\Omega$ is solid angle defining the detector acceptance, while ρ_s and d_s are the sample molecular density and thickness, respectively; $P(t_0, 2\vartheta, L_0, L_1)$ is the probability distribution that a given neutron leaves the moderator with a time delay t_0, travels from the moderator to the sample along a flight path L_0, is scattered at an angle 2ϑ, and finally travels from the sample to the detector along a flight path L_1.

The quantities $\Phi(E_0)$, $T(E_1)$ and $\mathrm{d}^2\sigma/\mathrm{d}\Omega\,\mathrm{d}\hbar\omega$ are the neutron flux at the incident neutron energy, the analyzer's energy transfer function and the double differential scattering cross section of the sample, respectively. The wide photon spectrum from the analyzer (atomic X-rays and nuclear gamma-rays) allows to use energy discrimination thresholds that improve the S/B, still guaranteeing an acceptable counting efficiency [19].

Eq. (10) represents only the signal component, i.e. assuming the absence of background. A more complete expression should contain background terms, as already discussed in a previous experimental paper [39]. The count rate in Eq. (10) can be expressed, for each recoiling mass present in the scattering sample, in terms of the NCP as (see Eqs. (2)–(5))

$$C(t,\langle 2\vartheta\rangle) = \sum_{i=1}^{n} \beta_i \cdot I_P \int_0^{\infty} \mathrm{d}E_0 \Phi(E_0) \int_0^{\infty} \mathrm{d}E_1 \times (1 - T(E_1))\delta(\tau)\sqrt{\frac{E_1}{E_0}}\frac{M_i b_i^2}{\hbar^2 q} F_{M,i}(y_i,\widehat{q}) \tag{14}$$

n being the number of different masses present scatterer. Standing Eq. (14), in the time of flight spectrum there will appear n recoil peaks (one per each recoiling mass) whose intensity is proportional to the number of atoms contained in the sample, weighted by the scattering cross-section. The time width and the shape of the recoil peak depends on the width and shape of $F(y, \hat{q})$, the uncertainties on the geometrical parameters (L_0, L_1 and 2ϑ), the time of flight (t) and the width and shape of the analyzer's transfer function $T(E_1)$. The width of $T(E_1)$ can be reduced, still maintaining an acceptable count rate, by applying the FCT, as already discussed in previous experimental papers [23,24].

References

[1] C. Andreani, D. Colognesi, J. Mayers, G.F. Reiter, R. Senesi, Adv. Phys. 54 (2005) 377.
[2] G.I. Watson, J. Phys.: Condens. Matter 8 (1996) 5955.
[3] P.C. Hohemberg, P.M. Platzman, Phys. Rev. 152 (1966) 198.
[4] R.N. Sinclair, M.C. Moxon, J.M. Carpenter, Bull. Am. Phys. Soc. 22 (1977) 101.
[5] H. Rauh, N. Watanabe, Nucl. Instr. and Meth. 228 (1984) 147.
[6] C.D. Bowman, R.G. Johnson, in: J. Faber Jr. (Ed.), AIP Conference Proceedings N° 89 Neutron Scattering, 1981.
[7] L. Cser, N. Kroó, P. Pacher, V.G. Simkin, E.V. Vasilieva, Nucl. Instr. and Meth. 179 (1981) 515.
[8] J.M. Carpenter, N. Watanabe, S. Ikeda, Y. Masuda, S. Sato, H. Rauh, Physica B 120 (1983) 126.
[9] N. Watanabe, in: Proceedings of the 1984 Workshop on High Energy Excitations in Condensed Matter, Los Alamos, February 13–15, LA-10227-C, vol. 1, 1984.
[10] M.P. Paoli, E.W.J. Mitchell, R.N. Sinclair, A.D. Taylor, in: ICANS VIII—Proceedings of the Eighth Meeting of the International Collaboration on Advanced Neutron Sources, RAL-85-110, Rutherford Appleton Laboratory, vol. 577, 1985.
[11] R.K. Crowford, in: ICANS IX—Proceedings of the Nineth Meeting of the International Collaboration on Advanced Neutron Sources, ISBN 3-907998-01-4, Swiss Institute for Nuclear Research, vol. 397, 1987.
[12] R.G. Johnson, C.D. Bowman, Phys. Rev. Lett. 49 (1982) 797.
[13] R.G. Johnson, Nucl. Instr. and Meth. A 163 (1985) 427.
[14] H. Rauh, S. Ikeda, N. Watanabe, Nucl. Instr. and Meth. 224 (1984) 469.
[15] C. Andreani, A. Pietropaolo, R. Senesi, G. Gorini, M. Tardocchi, A. Bracco, N.J. Rhodes, E.M. Schooneveld, Nucl. Instr. and Meth. A 481 (2002) 509.
[16] C. Andreani, A. D'Angelo, G. Gorini, S. Imberti, A. Pietropaolo, N. Rhodes, E. Schooneveld, R. Senesi, M. Tardocchi, Appl. Phys. A 78 (2003) 903.
[17] A. Pietropaolo, C. Andreani, A. D'Angelo, G. Gorini, S. Imberti, M. Tardocchi, N. Rhodes, E.M. Schooneveld, R. Senesi, in: Proceedings of the Eleventh International Symposium on Capture Gamma-Ray Spectroscopy and Related Topics, vol. 555, World Scientific, Singapore, 2003.
[18] M. Tardocchi, A. Pietropaolo, C. Andreani, A. Bracco, A. D'Angelo, G. Gorini, S. Imberti, R. Senesi, N.J. Rhodes, E.M. Schooneveld, Nucl. Instr. and Meth. A 526 (2004) 477.
[19] M. Tardocchi, G. Gorini, A. Pietropaolo, C. Andreani, R. Senesi, N. Rhodes, E.M. Schooneveld, Rev. Sci. Instr. 75 (2004) 4880.
[20] A. Pietropaolo, C. Andreani, A. Filabozzi, G. Gorini, N. Rhodes, R. Senesi, E. Schooneveld, M. Tardocchi, JINST 1 P04001, doi:10.1088/1748-0221/1/04/P04001.
[21] E. Perelli-Cippo, G. Gorini, M. Tardocchi, C. Andreani, A. Pietropaolo, R. Senesi, N.J. Rhodes, E.M. Schoonveld, Appl. Phys. A 83 (2006) 453.
[22] R. Senesi, C. Andreani, Z. Bowden, D. Colognesi, E. Degiorgi, A.L. Fielding, J. Mayers, M. Nardone, J. Norris, M. Praitano, N.J. Rhodes, W.G. Stirling, J. Tomkinson, C. Uden, Physica B 276–278 (2000) S189.
[23] E.M. Schooneveld, J. Mayers, N.J. Rhodes, A. Pietropaolo, C. Andreani, R. Senesi, G. Gorini, E. Perelli Cippo, M. Tardocchi, Rev. Sci. Instr. 77 (2006) 095103.
[24] A. Pietropaolo, C. Andreani, A. Filabozzi, E. Pace, R. Senesi, Nucl. Instr. and Meth. A 570 (2007) 498.
[25] J. Mayers, A.L. Fielding, R. Senesi, Nucl. Instr. and Meth. A 481 (2002) 454.
[26] A.L. Fielding, J. Mayers, Nucl. Instr. and Meth. A 480 (2002) 680.
[27] F. James, MINUIT minimisation package: reference manual, CERN Program Library, Geneva, 1994.
[28] D. Colognesi, A. Pietropaolo, R. Senesi, A.J. Ramirez Cuesta, Phys. Rev. B, 2007, accepted for publication.
[29] E. Perelli Cippo, G. Gorini, M. Tardocchi, O. Cremonesi, C. Andreani, A. Pietropaolo, R. Senesi, Z.A. Bowden, N.J. Rhodes, E.M. Schooneveld, IEEE Trans. Nucl. Sci. NS-52 (2005) 1092.
[30] G.B. West, Phys. Rev. 18 (1975) 263;
E. Pace, G. Salmé, G. West, Phys. Lett. B 273 (1991) 205.
[31] S.W. Lovesey, Theory of Neutron Scattering from Condensed Matter. 3rd ed., Oxford University Press, Oxford, 1987.
[32] V.F. Sears, Phys. Rev. B 30 (1984) 44.
[33] R.N. Silver, Phys. Rev. B 37 (1988) 3794.
[34] R.N. Silver, Phys. Rev. B 39 (1989) 4022.
[35] A.S. Rinat, Phys. Rev. B 36 (1987) 5171.
[36] H.A. Gersch, L.J. Rodriguez, P.N. Smith, Phys. Rev. A 5 (1972) 1547;
H.A. Gersch, L.J. Rodriguez, Phys. Rev. A 8 (1973) 905.
[37] H.R. Glyde, Phys. Rev. B 50 (1994) 6726.
[38] R. Senesi, D. Colognesi, A. Pietropaolo, T. Abdul-Redah, Phys. Rev. B 72 (2005) 054119.
[39] A. Pietropaolo, M. Tardocchi, E.M. Schooneveld, R. Senesi, Nucl. Instr. and Meth. A 568 (2006) 826.